

# PETROGRAPHIC CONTROLS ON ELECTRICAL PROPERTIES OF CORE SAMPLES FROM THE AWIBENGGOK GEOTHERMAL FIELD, INDONESIA

G. N. Boitnott<sup>†</sup> and J. B. Hulen<sup>‡</sup>

<sup>†</sup> New England Research Inc.

<sup>‡</sup> Earth and Geoscience Institute, U. Utah

## **Abstract**

The high-temperature (240-315 °C), Awibengkok geothermal system is hosted by porous, felsic to intermediate-composition, late Cenozoic volcanic rocks intensely altered to a variety of hydrothermal assemblages. We have determined experimentally, using representative samples from scientific corehole AWI 1-2, that the fundamental electrical properties of these cores are controlled not only by intrinsic porosity, but also by mineralogy.

Laboratory electrical impedance measurements on plugs of the AWI 1-2 cores, evaluated in the context of routine porosity determinations as well as petrographic and modal-mineralogic analysis, have enabled us to identify compositional and textural factors affecting the electrical characteristics of these rocks. Electrical formation factors ( $F$ ) of the cores follow a typical Archie porosity trend,  $F = \Phi^m$ , with  $m$  ranging between  $-2.6$  and  $-1.8$ . Aside from porosity we find that the volume fraction of illite and mixed-layer illite/smectite is the dominant control on the resistivity of these core samples. An empirical relationship incorporating porosity, illite, and chlorite concentrations is found to predict electrical resistivity to  $\pm 25\%$ , a significant improvement over the factor of 3 variation in predicted resistivity using porosity alone.

## **Introduction**

The Awibengkok reservoir consists of a sequence of hydrothermally altered lahars, tuffs and flow units. Over 1 km of continuous core was recovered from AWI 1-2, providing a unique resource for studying the reservoir rock. Induction log response observed in the sidetrack well AWI 1-2 ST#1 exhibits significant variations in resistivity in sections of the hole with apparently uniform lithology. While the temptation might be to attribute much of the log variation to porosity variation, the laboratory data suggests that this may not be the case. In order to better interpret the logs, a laboratory study is underway to develop a better understanding of the relative roles of porosity, mineralogy, rock type, and degree of alteration in controlling the electrical properties of the cores.

Sampling strategy for this study was motivated by the desire to develop a baseline dataset encompassing the major rock types and spanning the entire depth range of the AWI 1-2 corehole. Table 1 lists the samples reported here, along with their lithologies and bulk properties.

## Electrical Properties

Measurements of electrical impedance were made as a function of effective confining pressure, brine chemistry, and frequency. The primary brine used for laboratory testing was a 12000 ppm NaCl brine, being selected to approximate the salinity and dominant cationic composition of the brine in the reservoir. The resulting data set is referred to here as the routine data set, and will be compared later with specialized measurements designed to study dependence on brine conductivity.

The routine impedance data is presented in terms of the formation factor ( $F$ ), defined as the resistivity of the saturated rock normalized by the resistivity of the pore fluid. A summary plot of formation factors and "cementation exponents" [ $m = \log(F)/\log(\Phi)$ ] versus porosity is shown in Figure 1. While a clear trend in  $F$  with porosity is present (as is typical of most rocks), significant scatter is observed. This scatter can amount to a 50% variation in porosity for a given  $F$  or a factor of three variation in  $F$  for a given porosity. No systematic trends with depth or lithology are apparent.

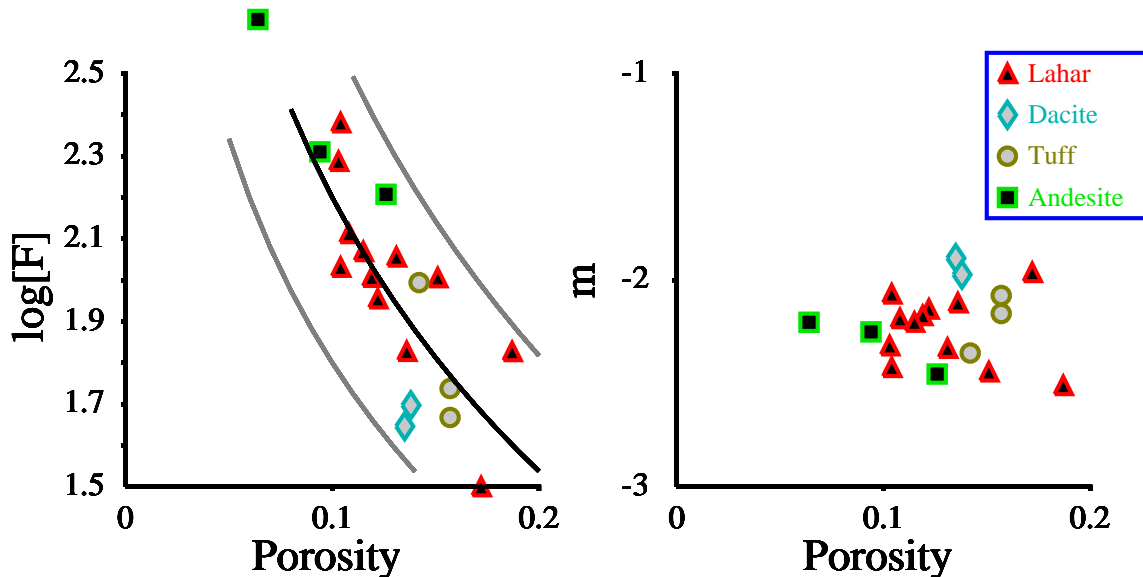


Figure 1: Logarithm of formation factors and cementation exponents versus porosity for brine saturated core plugs from AWI 1-2. The lines in the left hand figure represent  $m = -1.8, -2.2, -2.6$  respectively.

## Pressure, Temperature, and Frequency Dependence

While a detailed discussion of the pressure, temperature and frequency dependence of the electrical properties is beyond the scope of this paper, it is important to summarize the basic findings to provide the context for interpretation. Pressure and temperature dependence of  $F$  is in general relatively small, indicating that the observed scatter should be persistent at all depths. Frequency dependence is variable and can lead to relatively strong dispersions at logging frequencies. In some cases, there is a clear association with strong dispersion and the presence of disseminated sulfides in the sample. When the

disseminated sulfides are of relatively uniform size distribution, the expected narrow band response is observed, while for more complicated size distributions, the frequency dependence is more diffuse as is expected from theory (see Wong [1979], for background). Strong dispersions are also seen in some samples without concentrations of opaque minerals, indicating that clay related mechanisms are also present. Regardless of mechanism, the available data suggests that the observed dispersion, which can lead to a 20% reduction in  $F$  between 1 Hz and 10 kHz, is relatively insensitive to changes in pressure or temperature. Putting these observations into the context of this paper, the pressure, temperature, and frequency dependence are all second order effects on  $F$  when compared to the observed scatter between  $F$  and  $\Phi$  (which is the primary subject of discussion here).

### Mineralogic Controls

Illite and chlorite concentrations for selected samples were measured by whole rock XRD analysis. Cross-plotting various electrical impedance attributes with the available mineralogic data has yielded two suggestive trends. The cementation exponent  $m = \log(F)/\log(\Phi)$  exhibits weak correlations with illite and chlorite concentration (Figure 2). The data suggests that illite correlates with low  $F$  for a given porosity while chlorite exhibits the opposite association.

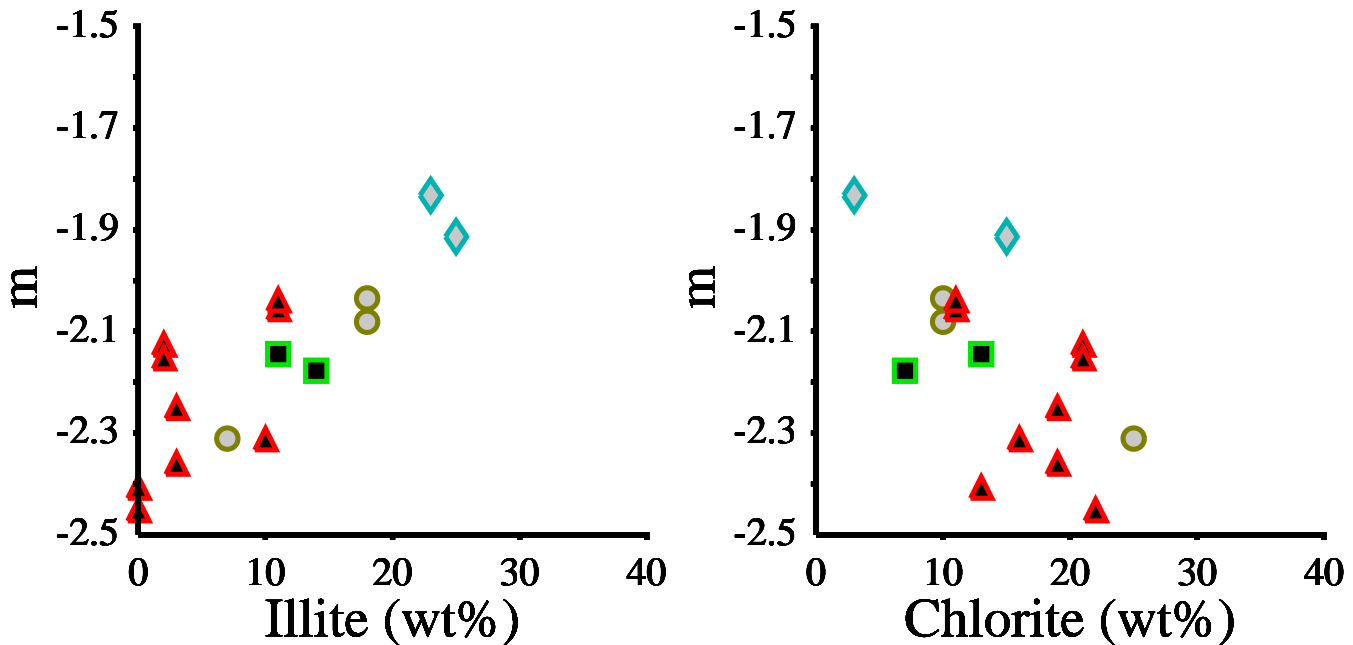
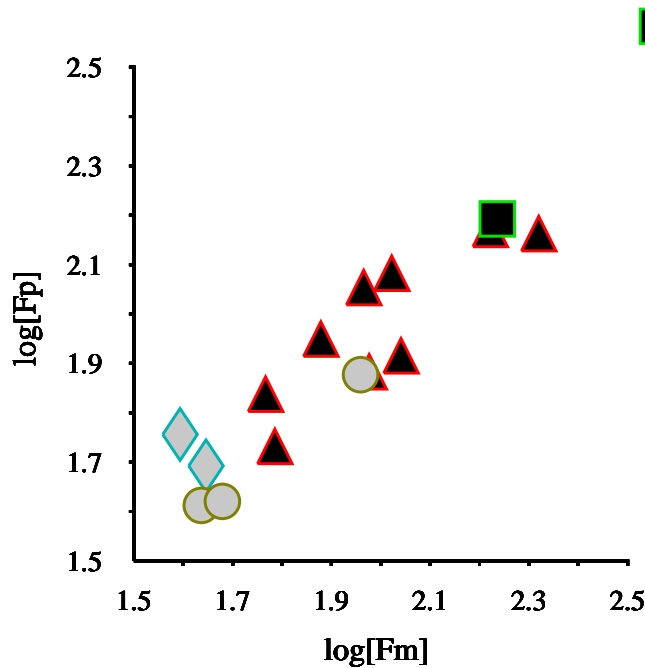


Figure 2: Cross plots of porosity,  $m$ , and illite and chlorite concentrations.

In order to begin quantifying the potential role of mineralogy in influencing the electrical properties, we start by searching to find a best fitting empirical relationship that minimizes the difference between measured and predicted values of  $F$ . Based on the observations in Figures 1 and 2, we chose the empirical form

$$F_p = \Phi^A + BI + CX + D \quad (1)$$

where  $\Phi$  is the porosity and  $I$  and  $X$  are the illite and chlorite contents in weight percent. We then find  $A$ ,  $B$ ,  $C$ , and  $D$  which minimize  $\sum(\log[F_m] - \log[F_p])^2$ , where  $F_m$  is the measured formation factor and  $F_p$  is the predicted formation factor. Figure 3 presents the results after allowing each term to contribute. Note that there is significantly less scatter between the predicted versus measured values than between the measured formation factors versus porosity, suggesting that the mineralogic controls on  $F$  are significant.



**Figure 3: Cross plots of  $\log[F_m]$  versus  $\log[F_p]$  based on equation 1 with  $A = -2.17$ ,  $B = -2.09$ ,  $C = 0.71$ , and  $D = 15.9$ .**

### The Effect of Brine Chemistry on Electrical Properties

The results in Figure 3 indicate that illite plays an important role in increasing the resistivity of these samples. One possible explanation is that the enhanced conductivity results from the surface conductivity of illite. Also a possibility is that there is a textural control related to illite, such as a decreased tortuosity as illite content increases. To independently test these ideas, a number of specialized measurements were made to constrain the amount of surface conduction in selected samples. Two types of experiments were

performed aimed at characterizing the brine dependence of the sample conductivity.

The first set of experiments involved analysis of closely spaced sub-cores, each saturated with a different brine. Three samples of various lithology were selected, based in part on their visual homogeneity. The subcores were oven dried (at 70 °C under vacuum for 24 hours) and submerged in jars of either NaCl or KCl brines of varying strength. Imbibition of brine was monitored by periodically weighing the samples. After a few days, when the imbibition of the brine had slowed to an undetectable level, the electrical properties of each sample were measured.

A summary plot of computed sample conductivities versus fluid conductivities is shown in Figure 4. A clear trend with brine concentration is seen, indicating general agreement with a Waxman and Smits [1968] type conductivity relationship. Brine composition does not appear to have a strong influence on electrical properties with no apparent difference between the NaCl and KCl saturated samples. Also included in Figure 3 are results from the routine data set, indicating that the imbibition method of saturation has not biased the result. The results for each sample can be parameterized by the relation

$$C_{sample} = C_{surface} + C_{brine}/F^* \quad (2)$$

where  $C_{sample}$ ,  $C_{surface}$ , and  $C_{brine}$  are the sample, surface, and brine conductivities respectively, and  $F^*$  is a modified formation factor describing the resistivity of the porous system in parallel with a surface conductivity element. Similarly, a surface conductivity corrected Archie exponent  $m^*$  can be defined as [ $m^* = \log(F^*)/\log(\Phi)$ ].

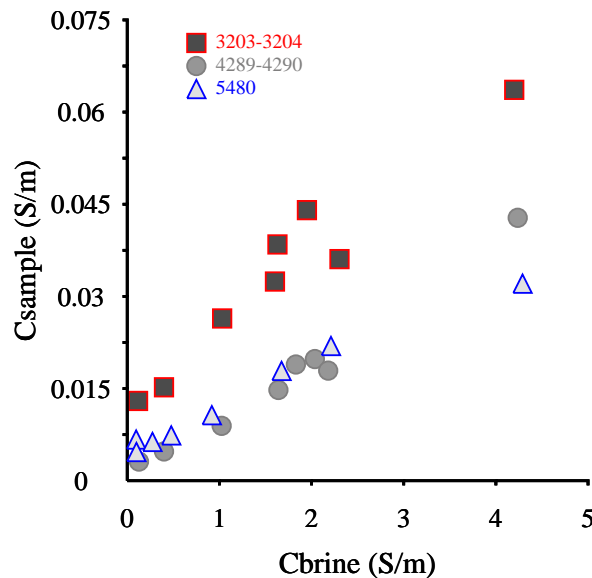


**Figure 4: The effect of brine chemistry and strength of the electrical conductivity and formation factor of three hydrothermally altered samples from AWI 1-2.**

In order to supplement this data set, a second procedure was used to obtain the same sort of information on individual sub-cores. Saturated samples from the routine data

set were submerged in a large volume of tap water, with the tap water being refreshed periodically. The tap water conductivity was monitored to indicate leaching of salts from the samples. Once no further leaching was detected, the samples were retested. Assuming the samples behave according to Equation 2, a constraint on  $C_{surface}$  is obtained. From these two data sets,  $C_{surface}$ ,  $F^*$ , and  $m^*$  were computed and are presented in Table 2.

Plotting  $C_{surface}$  versus illite content (Figure 5) produces a suggestive trend indicating that a surface conductivity contribution is influenced by illite concentration. Plotting  $F^*$  and  $m^*$  versus porosity however, we still do not produce well defined trends (Figure 6). This implies that the porosity and/or textural contribution to the sample resistivities is intrinsically variable. A weak decrease in  $m^*$  with increasing porosity is suggested by the data.

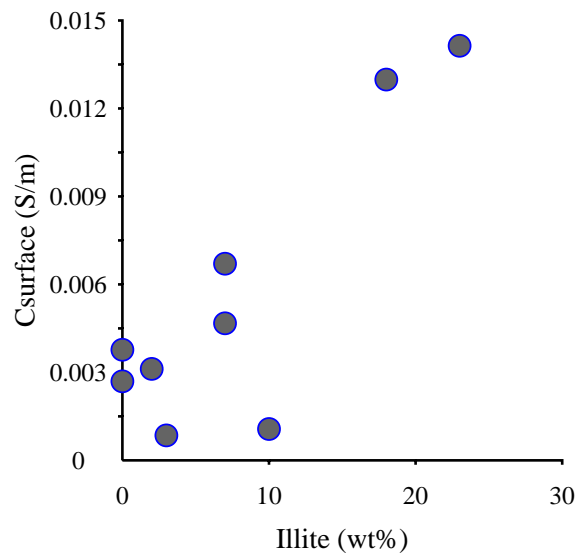


**Figure 5: Inferred  $C_{surface}$  versus weight percent illite for selected samples from AWI 1-2 (see Table 2).**

A simple physical model that results is that of a porous matrix with brine conductivity defined by an Archie relationship  $F^* = \Phi^{m^*}$  with  $m^*$  weakly dependent on porosity in parallel with a surface conductivity element (independent of brine concentration) which is proportional to the abundance of illite in the sample. However, this interpretation cannot fully explain the success of Equation 1 in predicting  $F$  to  $\pm 25\%$ . While surface conduction enhanced by illite appears to be an important conduction mechanism, there also appears to be a textural component, again apparently associated with illite content, that plays a more significant role in influencing  $F$ .

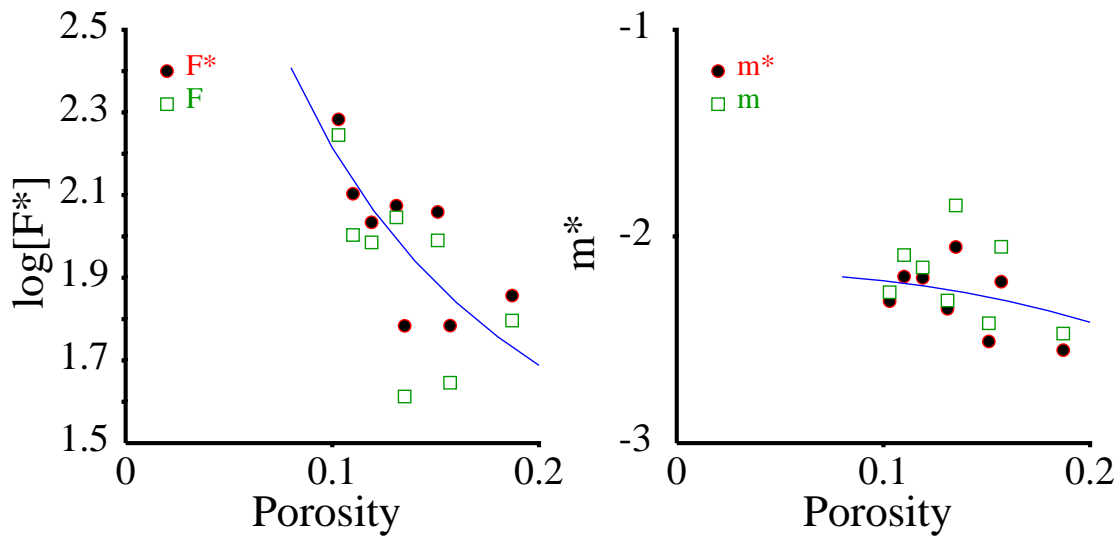


**Figure 6: Logarithm of  $F^*$  and  $m^*$  versus porosity for selected samples from AWI 1-2. Also for reference,  $F$  and  $m$  are plotted for the same samples (squares) and the curve  $F = \Phi^{-2.17} + 15.9$ , which is the non-mineralogic terms from Equation 1 (see Figure 3).**

## Conclusions

We have found that the electrical properties of core samples from AWI 1-2 generally follow an Archie type relationship with porosity, but that significant scatter in the relationship exists. An empirical model of  $F$  dependent on porosity, illite, and chlorite content significantly improves the prediction of  $F$ . Independent experiments also indicate a surface conductivity which is roughly proportional to illite content, but this surface conductivity term cannot in itself explain the empirically observed dependence of  $F$  on illite. This indicates that textural controls on  $F$ , which appear in some way to be associated with the abundance of illite and chlorite, must lead to much of the observed scatter in electrical properties. Better knowledge of this relationship will lead to enhanced interpretation of induction logs and exploration data.

## References

- Waxman, M. H., and Smits, L. J. M., Electrical conductivities in oil-bearing shaly sandstones, Transactions AIME, v 243, part II, 107-122, 1968.
- Wong, J., An electrochemical model for the induced-polarization phenomena in disseminated sulfide ores, Geophysics, v. 44, p. 1245-1265, 1979

Sample	Depth m	Lithology	Porosity	$F'$
2520_0a	768.10	Lahar	0.151	95
2541_7a	774.71	Lahar	0.187	61
3035_0a	925.07	Dacite_Autobreccia	0.135	39
3100_1a	944.91	Dacite_Autobreccia	0.138	44
3204_1b	976.61	Tuff	0.156	43
3204_1b	976.61	Tuff	0.157	44
4072_7a	1241.36	Lahar	0.122	78
4072_7b	1241.36	Lahar	0.136	58
4125_3a	1257.39	Lahar	0.103	167
4125_4a	1257.42	Lahar	0.104	209
4218_0a	1285.65	Lahar	0.108	126
4290_0b	1307.59	Lahar	0.104	98
4290_2a	1307.65	Lahar	0.119	92
4290_3a	1307.68	Lahar	0.115	104
4504_4a	1372.94	Andesite	0.191	362
4789_0a	1459.69	Andesite	0.126	151
5091_1a	1551.77	Lahar	0.172	31
5110_1a	1557.59	Andesite	0.094	172
5480_0b	1670.3	Tuff	0.142	91
5513_6a	1680.55	Lahar	0.132	110

Sample	Porosity	Illite <sup>†</sup> wt%	Chlorite wt%	$F^*$	$m^*$	$C_{surface}$ mS/m
2520_0a	0.151	0	13	114.6	-2.51	2.69
2541_7a	0.187	0	22	71.9	-2.55	3.77
3035_0a	0.135	23	3	60.8	-2.05	14.1
3203-3204 <sup>‡</sup>	0.157	18	10	60.8	-2.22	13.0
4125_4a	0.104	3	19	192.0	-2.31	0.85
4289-4290 <sup>‡</sup>	0.119	2	21	108.2	-2.20	3.12
5480 <sup>‡</sup>	0.110	7	25	126.8	-2.19	5.65
5513_6a	0.131	10	16	118.7	-2.35	1.07

<sup>†</sup> includes mixed layer Illite/Smectite  
<sup>‡</sup> data from multiple samples